

999 **Supplementary Materials and Methods**

1000 *Subjects*

1001 Four adult subjects (2 men, 2 women) with BVL participated in this study. Inclusion criteria  
1002 included age 22-90 years, summed responses to warm/cool caloric vestibular stimulation below  
1003 10°/s per ear, MRI and CT imaging confirming normal ear and vestibular nerve anatomy, and  
1004 sufficient hearing in the contralateral ear to support communication. All subjects must be  $\geq 12$   
1005 months post-onset and must have completed  $\geq 6$  months of vestibular rehabilitation therapy  
1006 exercises while off vestibular-suppressant medications. Exclusion criteria included vestibular  
1007 areflexia etiologies outside of the labyrinth, medical conditions that could impede a subject's  
1008 ability to complete testing, or any medical contraindication to the planned surgery.

1009 Prior to enrollment, subject MVI001 (male, 61 years old on entry into the study) received  
1010 intravenous gentamicin for 14 days in 2012 for a leg injury. Post-aminoglycoside treatment, the  
1011 subject reported symptoms of profound BVL which persisted for over 4 years following a plateau  
1012 of compensation from rehabilitation therapy. The subject was implanted with the MVI system in  
1013 the left ear in August 2016. Subject MVI002 (male, 57 years old) suffered from vertigo, imbalance,  
1014 and oscillopsia in 2006 following spinal surgery. The subject was further treated with bilateral  
1015 intratympanic streptomycin in 2007 and experienced symptoms consistent with BVL thereafter.  
1016 On presentation to Johns Hopkins in 2016, the subject reported an incomplete recovery from  
1017 vestibular rehabilitation exercises started in 2010. He underwent implantation of an MVI  
1018 stimulator in his left ear in November 2016. Subject MVI003 (female, 63 years old) suffered from  
1019 symptoms of BVL after 7 days of intravenous gentamicin treatment for a kidney stone urosepsis  
1020 in 2015. The subject performed vestibular physical therapy for over a year without sufficient

1021 recovery and was implanted in her left ear with the MVI in February of 2017. Subject MVI004  
1022 (female, 62 years old) was treated for 14 days with gentamicin after an operation to treat a pelvic  
1023 abscess in 2015. After the onset of BVL symptoms, she participated in vestibular therapy, which  
1024 incompletely alleviated her symptoms. This subject's left ear was implanted with an MVI  
1025 stimulator in December 2017.

#### 1026 *Surgery*

1027 Each subject was implanted with the receiver/stimulator component of a Labyrinth Devices MVI  
1028 system in the left ear via a post-auricular incision and transmastoid approach similar to that  
1029 typically used for cochlear implantation or labyrinthectomy, except that no entry was made into  
1030 the cochlea and instead four ~0.6-0.75 mm diameter openings were made into the labyrinth (in the  
1031 anterior and horizontal semicircular canal ampullae and in the thin segment of the posterior canal  
1032 near the ampulla and near the common crus), via which electrodes were inserted. Bone pate was  
1033 applied around the points where the electrode arrays entered the labyrinth. The receiver/stimulator  
1034 (Figure 2) was secured with suture in a bone well and sub-periosteal pocket in the post-auricular  
1035 region. All surgeries were performed on an outpatient basis at the Johns Hopkins Hospital or Johns  
1036 Hopkins Outpatient Center by the same surgeon (CCDS). Two subjects (MVI002 and MVI003)  
1037 were discharged directly from the post-anesthesia recovery unit within 2 hours after surgery; the  
1038 other two stayed for extended observation until the next morning and were then discharged to a  
1039 nearby hotel.

#### 1040 *3D eye movement recording*

1041 Eye movements were recorded using 3DBinoc™ video-oculography (VOG) goggles (Labyrinth  
1042 Devices, LLC), which use a single camera to track binocular 3D eye position while illuminating  
1043 the subject's eyes using infrared LEDs (allowing ocular tracking without visible light). The  
1044 goggles assay horizontal and vertical components of eye position via pupil tracking and measure  
1045 torsional angular position using iris pattern template matching (44). Custom VOG software  
1046 acquired 3D angular eye position data at 100-180 frames-per-second with a peak-to-peak noise  
1047 floor of 0.15°, 0.07°, and 0.06° for the torsional, vertical, and horizontal 3D components,  
1048 respectively. The goggles use a pair of IR-pass optical filter insets to block the subject's view of  
1049 visible light during data acquisition. 3DBinoc™ goggles interface with a host PC through a  
1050 galvanically isolated USB connection and directly connect to each subject's PCU for stimulus  
1051 trigger synchronization.

#### 1052 *Data analysis*

1053 The 3DBinoc™ system reports 3D angular position data as gaze direction (i.e., horizontal and  
1054 vertical position of the pupil) and torsion around the eye's line-of-sight. We processed raw angular  
1055 position data traces with third-order median filters to recover VOG tracking dropouts. 3D angular  
1056 position data were converted to rotation vectors (47) and filtered with second or third order  
1057 Savitsky-Golay filters (76) for high frequency noise rejection. We first computed 3D angular  
1058 velocity in X ('roll'), Y ('pitch'), and Z ('yaw') head-fixed coordinates then transformed angular  
1059 velocity data into anatomic canal coordinates by applying a -45° passive reorientation of the head-  
1060 fixed coordinate system about the yaw axis (45, 77, 78).

1061 Nystagmus quick phases were detected and excised using an eye acceleration threshold. Spline  
1062 interpolation across excised segments produced smooth slow phase eye velocity traces. We

1063 computed cycle averages after removing trails corrupted by blinks or drops in pupil/iris tracking.  
1064 Eye position data collected during adaptation to MVI activation were processed with custom  
1065 software that fit a least-squares linear model to slow phase responses between auto-detected quick  
1066 phases. The slope of the fitted line for each 3D component and corresponding angular position  
1067 values was used to compute 3D angular velocity using standard rotational kinematic techniques  
1068 (78).

#### 1069 *Electrode characterization and activation*

1070 For pre-activation electrical stimulation characterization measurements, a 200pps pulse train was  
1071 delivered to each electrode contact (with pulse train duration 200ms and inter-train-interval  
1072 300ms) to assay responses at each tested current level. Pulse train stimuli were first used to  
1073 characterize perceptual thresholds, VOR thresholds, and maximum current levels for each tested  
1074 electrode/phase duration combination. These data were used to generate 10 (MVI001 and  
1075 MVI002) or 7 (MVI003 and MVI004) current amplitudes spanning the VOR threshold and  
1076 maximum current level to assay acute 3D VOR responses during MVI stimulation (Table S1).

1077 Following electrode characterization, a stimulation parameter set (including electrode contact,  
1078 current amplitude, and phase duration) was programmed into the subject's PCU for each canal.  
1079 Stimuli were chosen to optimize evoked VOR magnitude and response alignment with target canal  
1080 anatomic axes (Table S2). Device activation (including adaptation to baseline tonic electrical  
1081 stimulation) was performed with the subject on a bite-block in total darkness. Each active electrode  
1082 was programmed to provide biphasic, charge balanced current pulses at 100pps on all three active  
1083 canal channels.

1084 The nystagmus evoked by the onset of stimulation was measured in darkness for 1 minute, after  
1085 which the lights in the experimental room were turned on and the IR-pass filters removed from the  
1086 3DBinoc™ goggles for 4 minutes. When in light the subject was instructed to focus on an Earth-  
1087 fixed target to promote adaptation to prosthetic baseline stimulation via retinal slip error signals  
1088 during the evoked nystagmus. This procedure (1 minute in darkness to assay vestibular nystagmus  
1089 responses and 4 minutes to promote adaptation) was repeated until all components of the  
1090 spontaneous nystagmus in darkness were  $<5^{\circ}/s$ . Subjects MVI002, MVI003, and MVI004 were  
1091 later adapted to a 150pps baseline pulse rate on the same day.

#### 1092 *Virtual head rotation (prosthesis-only) stimulation*

1093 For experiments examining responses solely driven by prosthetic input, the PCU was programmed  
1094 to bypass gyroscopic input from the HWU and provide ‘virtual’ head motion signals processed by  
1095 the subject’s PCU. The device communicated with the implanted stimulator to provide a sequence  
1096 of pulsatile stimuli encoding head rotations according to each canal’s stimulation parameters  
1097 describing relationships between head velocity and both pulse rate and pulse amplitude for each  
1098 active electrode (Table S3). These stimuli were delivered with the subject in darkness and their  
1099 head stationary on a custom bite-block to prevent visual, latent vestibular, or cervico-ocular reflex  
1100 responses from influencing recorded eye movements.

#### 1101 *Rotary chair testing*

1102 An Earth-vertical rotary chair (NeuroKinetics, Inc., Pittsburgh, PA) was used to provide whole  
1103 body, *en bloc* sinusoidal rotations in darkness using frequencies between 0.1–2Hz at  $100^{\circ}/s$  peak  
1104 velocity. Rotatory testing was performed both pre-operatively and post-operatively before any

1105 electrical stimulation to assay changes to mechanical vestibular function due to surgical  
1106 procedures. After activation of the MVI system, testing was completed in the following two  
1107 conditions: a) with the device set to provide pulsatile stimulation that modulated according to  
1108 parameters programmed into the subject's PCU ("Modulation ON") and b) with the PCU set to  
1109 provide non-modulating, constant-rate and -amplitude tonic stimulation on each active canal  
1110 electrode ("Modulation OFF").

1111

### 1112 *Subject stimulus parameter mappings*

1113 The MVI encodes 3D head velocity via modulation of pulse rate and/or pulse amplitude of the  
1114 adapted electrical stimulus delivered to each active canal electrode. For each active contact within  
1115 a canal ampulla, a head velocity-to-pulse rate and head velocity-to-pulse amplitude mapping was  
1116 programmed into the subject's PCU to update pulsatile stimulation parameters and encode 3D head  
1117 rotation components about each anatomic canal axis. Mappings were programmed as either:

#### 1118 1) Flat

1119 Where pulse rate or amplitude is set to a single value that does not change with head  
1120 velocity.

#### 1121 2) Piecewise-Linear

1122 A two-segment, piecewise-linear map constructed by mapping the head velocity input  
1123 range from  $[-400^\circ/\text{s}, 0^\circ/\text{s}, +400^\circ/\text{s}]$  to the minimum, baseline, and maximum pulse rate or  
1124 amplitude determined during electrode characterization.

1125 3) Sigmoidal

1126 A non-linear mapping created using a hyperbolic tangent function to mimic the response  
1127 dynamics of primary vestibular afferents in non-human primates (30, 31, 79) defined by:

$$Pulse(t) = 0.5 * (P_{MAX} - P_{MIN}) * \left( 1 + \tanh \left( X + C_{RATE} * \left( \frac{v(t)}{v_{MAX}} \right) \right) \right) + P_{MIN}$$

1128

1129 and

$$X = \operatorname{atanh} \left( 2 * \frac{P_{BASELINE} - P_{MIN}}{P_{MAX} - P_{MIN}} - 1 \right)$$

1130

1131 Where:

1132  $Pulse(t)$  = Mapping describing either pulse-amplitude- or pulse-rate-modulation of prosthetic  
1133 stimulation as a function of head velocity.

1134  $v(t)$  = Input head velocity waveform. This can be generated either via measurements made using  
1135 the 3-axis gyroscope sensors in the subject's HWU or generated by a galvanically isolated  
1136 computer with the subject's head stationary.

1137  $v_{Max}$  = Maximum input head velocity magnitude. Set to 400°/s for all subjects. The head velocity  
1138 input range is set to  $[-v_{Max}, v_{Max}]$ .

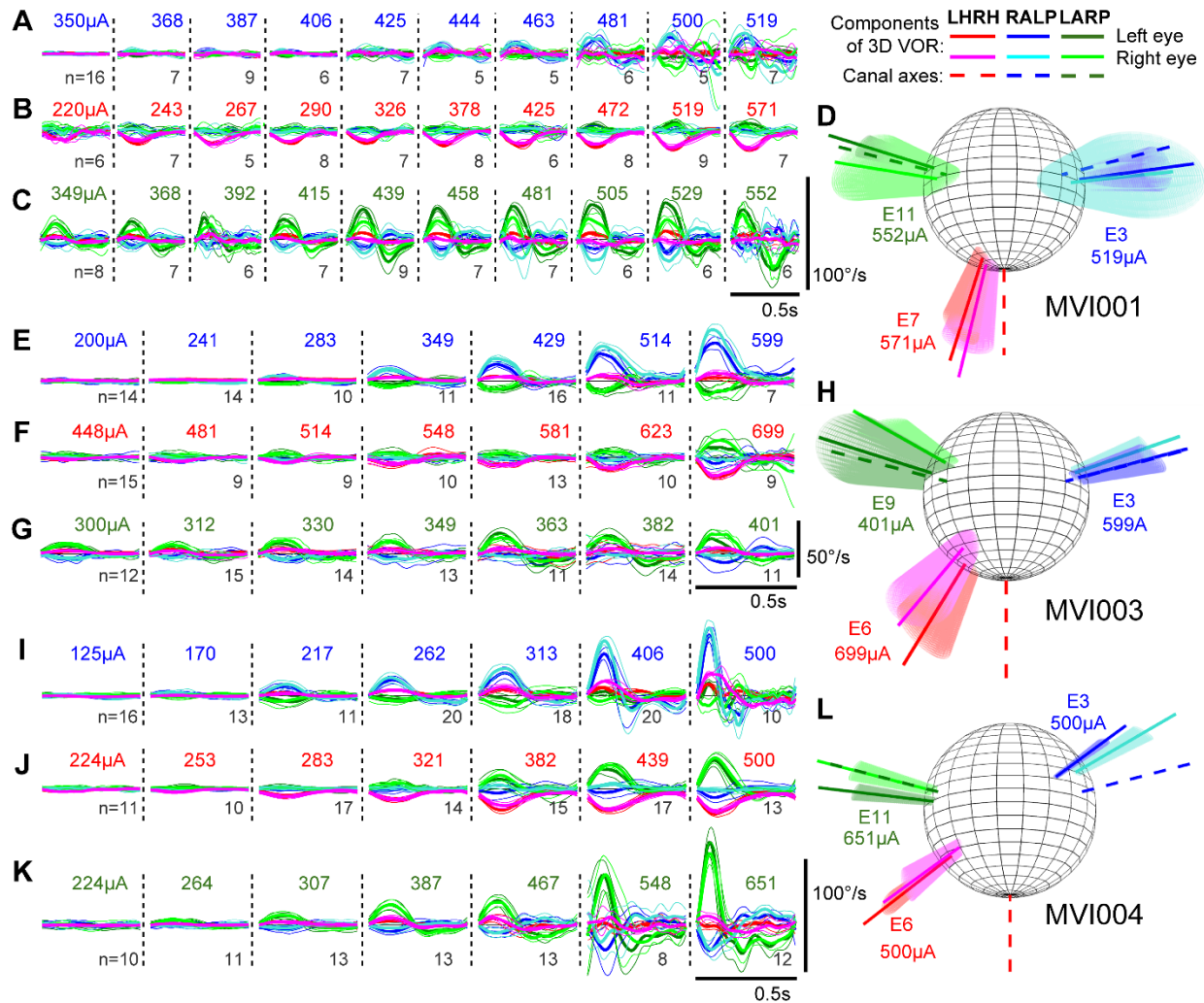
1139  $P_{Baseline}$  = Pulse rate or amplitude used when the subject's head is stationary (i.e., 0°/s)

1140  $P_{Max}$  = Maximum pulse rate or amplitude used to encode the maximum input head velocity ( $v_{Max}$ ).

1141  $P_{Min}$  = Minimum pulse rate or amplitude used to encode the minimum input head velocity ( $-v_{Max}$ ).

1142 C = Compression factor defining the slope of the head velocity-to-pulse rate or -pulse amplitude  
1143 curve.





1144  
 1145  
 1146  
 1147  
 1148  
 1149  
 1150  
 1151  
 1152  
 1153  
 1154  
 1155  
 1156  
 1157

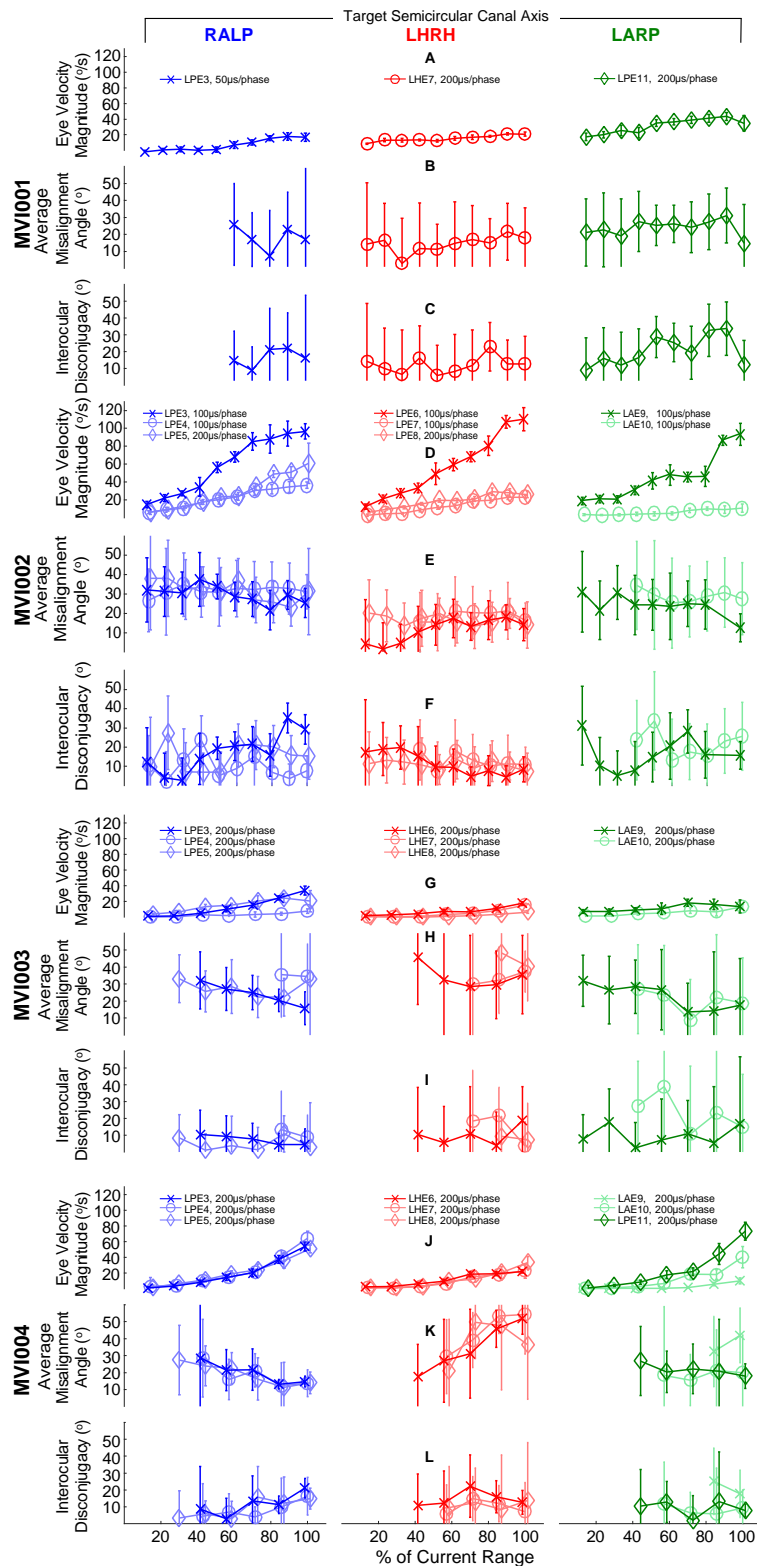
**Figure S1. Binocular 3D Responses from subjects MVI001, MVI003, and MVI004.**

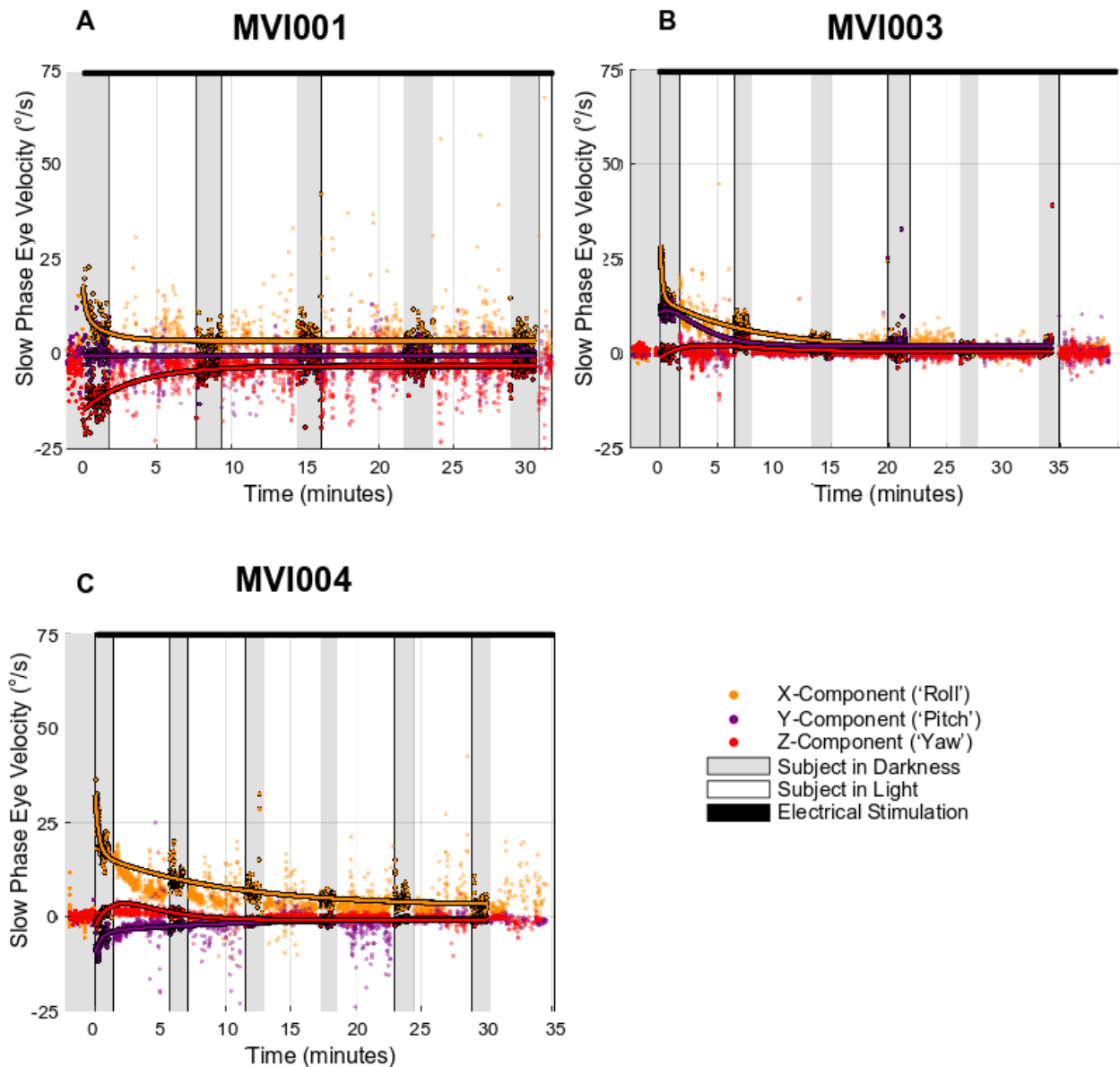
Binocular cycle averaged 3D slow phase eye velocity traces in response to 2Hz, 40% duty cycle pulse trains oscillating between 200pps (200ms) and 0pps (300ms). Data are shown as mean±SD for n cycles. Pulse trains were delivered to isolated electrode contacts on subjects MVI001 (A-D), MVI003 (E-H), and MVI004 (I-L). For subject MVI001, pulse trains delivered to (A) electrode E3 using 50μs/phase biphasic current pulses, (B) electrode E7 using 200μs/phase, and (C) electrode E11 using 200μs/phase pulses produced canal specific responses. The axis of rotation of the eye movement evoked by the maximum current level for each of the three electrodes is plotted in (D). When tested on electrodes (E) E3, (F) E6, and (G) E9 using 200μs/phase current pulses, subject MVI003 produced eye movements well aligned with the LP and LA canals. Stimuli delivered to the LH canal produced a response consistent with activation of the LH ampullary nerve and spurious stimulation of the LA canal, depicted graphically in (H). Lastly, subject MVI004 produced similar responses when tested on electrodes (I) E3, (J) E6, and (K) E11 using 200μs/phase current pulses, where stimulation of electrode contacts in the LA and LP ampullae produced well aligned responses, while stimulation in the horizontal canal produced a mixed LHRH/LARP response.

1158  
 1159  
 1160  
 1161  
 1162  
 1163  
 1164  
 1165  
 1166  
 1167  
 1168  
 1169  
 1170  
 1171  
 1172  
 1173  
 1174  
 1175  
 1176  
 1177  
 1178  
 1179  
 1180  
 1181  
 1182  
 1183  
 1184  
 1185  
 1186  
 1187  
 1188  
 1189  
 1190  
 1191  
 1192  
 1193  
 1194  
 1195  
 1196  
 1197  
 1198  
 1199  
 1200  
 1201  
 1202  
 1203  
 1204  
 1205  
 1206  
 1207

**Figure S2. Current fitting summaries for subjects MVI001, MVI002, MVI003, and MVI004.**

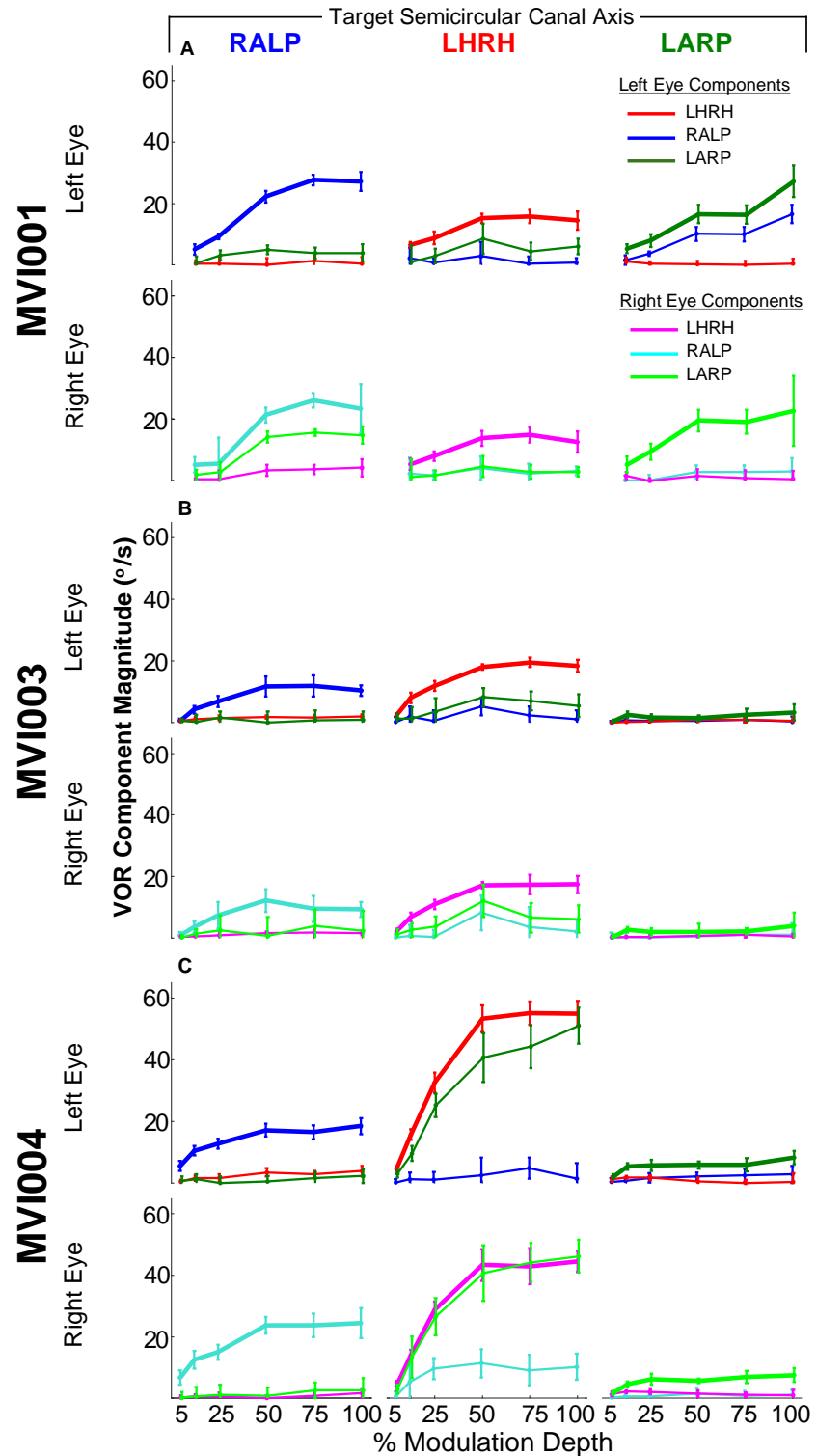
Vestibulo-ocular reflex eye movement velocity magnitude, misalignment angle and interocular disconjugacy for responses to electrical stimulation delivered individually via each stimulating electrode in each subject's implanted (left) labyrinth. Data are shown as mean±SD for n=5 to 20 (median 12) cycles. Electrode contacts chosen for continuous motion-modulated stimulation for device activation are bolded while data collected from the remaining contacts are faded. The misalignment angle plotted as a function of current amplitude intensity, where misalignment is computed as the angle between the mean binocular axis of rotation and the intended canal axis of rotation. Binocular disconjugacy is plotted as the angle between the mean VOR rotation axes of the left and right eye as a function of current intensity. (A-C) MVI001 was only thoroughly tested on electrodes E3, E7, and E11 in the LP, LH, and LA canals respectively due to restricted time. (D-F) Subject MVI002 produced robust responses when assayed using the electrodes on the tip of each electrode shank (i.e., electrode E3 in the LP canal, E6 in the LH canal and E9 in the LA canal). (G-I) Subject MVI003 produced eye movements that approximated the target canal axis of rotation, with overall smaller amplitude eye velocities compared to MVI002. (J-L) MVI004 produced strong eye movements during stimulation of electrodes in the LP and LA canals (G, left and right) that were consistent with selective stimulation of their respective ampullary nerve branches. Stimulation of electrodes in the LH canal (H, middle) produced eye movements with a large LARP component (as seen in Figure S1J). All stimulus parameters are listed in Table S1. Responses with peak eye velocities <5°/s were too small to provide accurate estimates of misalignment or interocular disconjugacy and are not displayed in the figure.

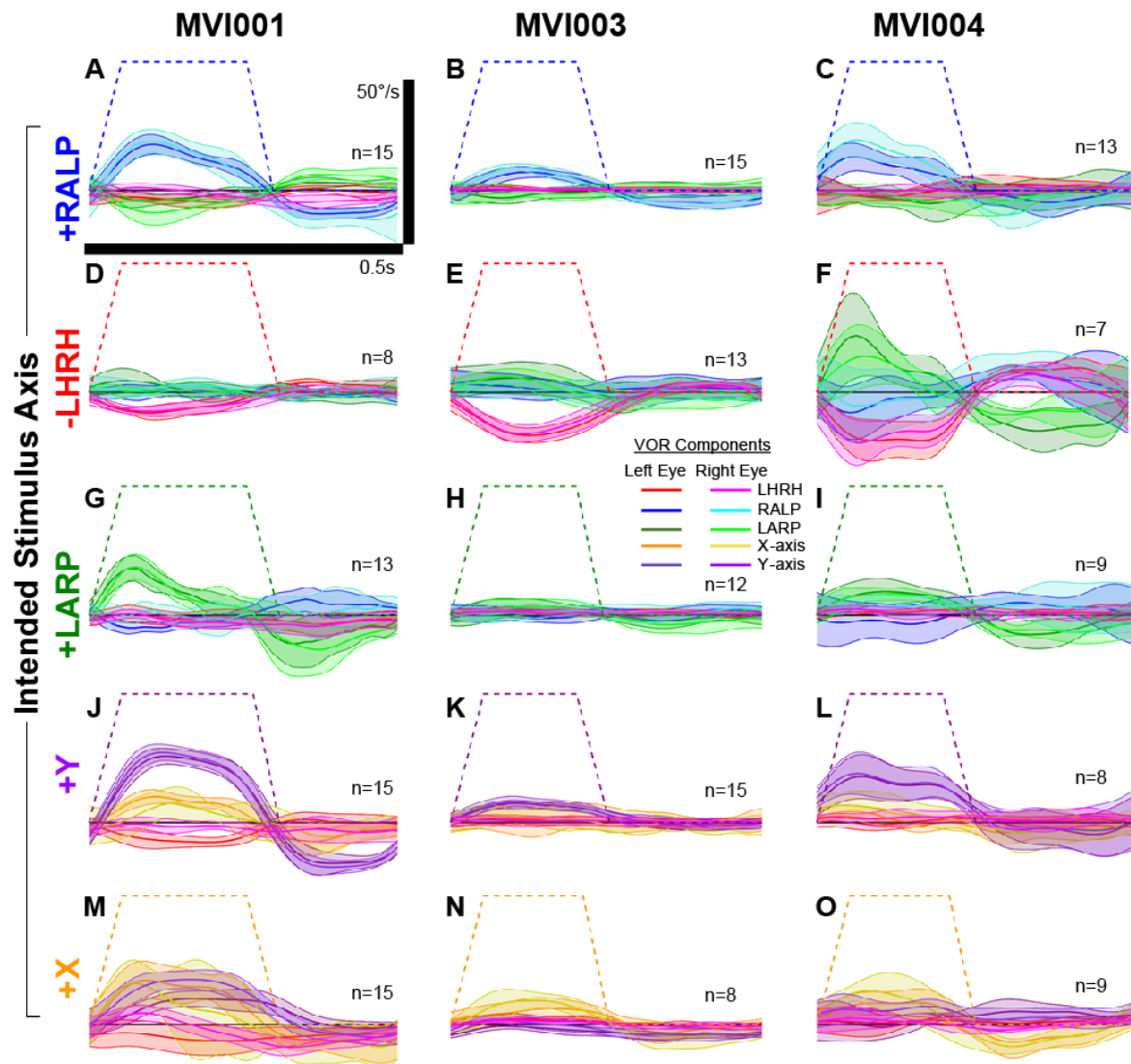




1208  
 1209 **Figure S3. MVI001, MVI003, and MVI004 adaptation to constant rate and current electrical stimulation.**  
 1210 Subjects (A) MVI001, (B) MVI003, and (C) MVI004 all produced nystagmus responses to the onset of prosthetic  
 1211 vestibular stimulation delivered to electrodes in each canal that decayed to imperceptible levels within ~30 minutes.  
 1212 (A) Subject MVI001 produced a brisk nystagmus that decayed within the first minute in darkness. (B) Subject  
 1213 MVI003 produced a positive roll component that decreased rapidly within the first minute in darkness. The subject  
 1214 also produced a positive pitch component in addition to the positive roll component, consistent with a higher level of  
 1215 evoked activity in the LP ampullary nerve branch relative to the LA nerve group. Also, this subject and subject (C)  
 1216 MVI004 produced a nystagmus with a small negative ( $\sim -3^\circ/\text{s}$ ) yaw component that reversed direction within the first  
 1217 minute in darkness. This finding is consistent with reversal phases of evoked nystagmus during sustained vestibular  
 1218 stimulation. Each point represents one slow phase nystagmus segment. Second order exponential fits of slow phase  
 1219 velocity data acquired in darkness revealed dominant roll time constants of 1.5, 7.8, and 9.6 minutes (RMSE = 3.1,  
 1220 1.7, and 2.8 $^\circ/\text{s}$ ) for MVI001, MVI003, and MVI004, respectively.  
 1221

1222 **Figure S4. Eye movement responses to 2Hz sinusoidal head velocity waveforms (MVI001, MVI003,**  
1223 **and MVI004).** Excitatory half-cycles of eye movement responses to “virtual head rotation” prosthesis-only  
1224 stimulation using 2Hz sinusoidal modulation targeting one electrode in each canal reveal ability to drive canal-  
1225 specific VOR responses after 8 wk of motion-modulated prosthetic stimulation. All data were collected with the  
1226 subject’s head stationary on a bite-  
1227 block and the test environment  
1228 darkened by occluding the subject’s  
1229 vision with visible-light blocking  
1230 filters and turning off the  
1231 experimental room lights. Target  
1232 canal components are bolded in  
1233 each figure. Data are shown as  
1234 mean±SD for n=7 to 20 (median 16)  
1235 cycles. (A) Subject MVI001  
1236 produced stable VOR responses that  
1237 grew in magnitude with modulation  
1238 intensity. VOR responses tended to  
1239 rotate about an axis that closely  
1240 approximated the target anatomic  
1241 canal axis, except during RALP  
1242 stimulation in the right eye and  
1243 LARP stimulation in the left eye.  
1244 (B) Testing subject MVI003 with  
1245 virtual head velocity sinusoids  
1246 produced eye movements  
1247 resembling the intended canal axes  
1248 of rotation, though with lower  
1249 amplitude peak eye velocities  
1250 compared to subject’s MVI001 and  
1251 MVI002. Modulation of the current  
1252 stimulus on electrode E9 in the LA  
1253 canal (B, right) produced small  
1254 amplitude eye movements when  
1255 tested at 100% modulation depth  
1256 (Left eye: 3.4±2.6°/s, Right eye:  
1257 4.0±4.2°/s). (C) Subject MVI004  
1258 produced 3D responses that  
1259 approximated the intended anatomic  
1260 canal axis of rotation during  
1261 modulation of the electrical stimulus  
1262 delivered to electrodes E3 in the LP  
1263 canal (C, left) and E11 in the LA  
1264 canal (C, right). During modulation  
1265 of electrode E6 in the LH canal (C,  
1266 middle), the intended 3D component  
1267 aligned with the subject’s LHRH  
1268 axis (red and pink traces) grew with  
1269 modulation depth with an  
1270 unintended LARP component (dark  
1271 and light green) that was likely due  
1272 to co-activation of the LA nerve  
1273 branch.



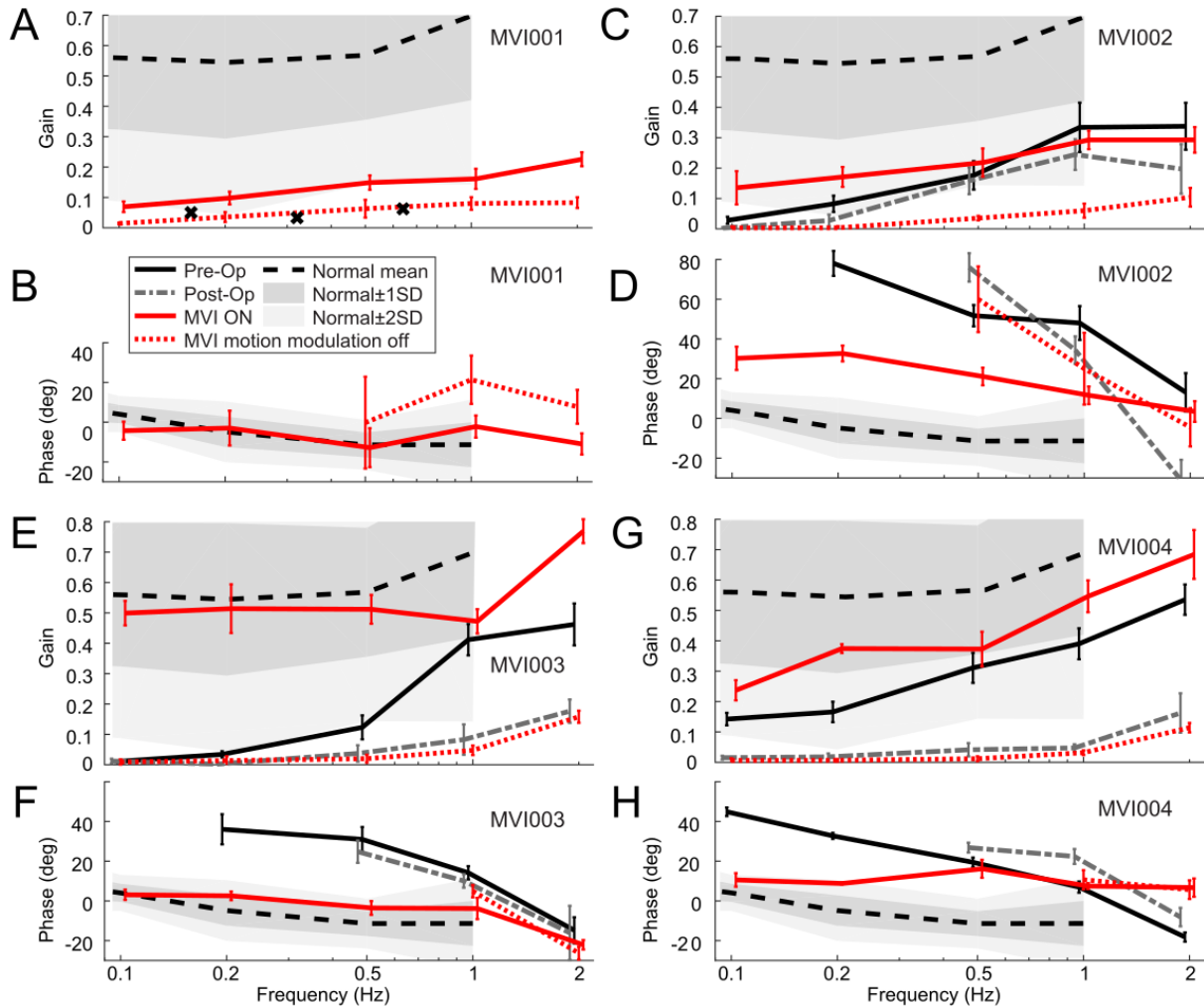


1275  
 1276  
 1277  
 1278  
 1279  
 1280  
 1281  
 1282  
 1283  
 1284  
 1285  
 1286  
 1287  
 1288

**Figure S5. Responses to combinations of canal electrode approximate non-canal axes of rotation (MVI001, MVI003, and MVI004).**

Mean±SD 3-dimensional vestibulo-ocular reflex velocity for  $n$  cycles of responses to coordinated stimulation via multiple electrodes can approximately encode arbitrary head rotation axes (MVI001, MVI003, and MVI004). (A,D,G,J,M) For subject MVI001 combining modulation of electrodes E3 and E11 out of phase produced a predominantly vertical eye movement (J), while modulating E3 and E11 in-phase (M) evoked a binocular eye movement with comparable positive vertical and torsional eye velocities (which is a principally RALP eye movement when converted into anatomic canal coordinates). (B,E,H,K,N) MVI003 produced eye velocities well aligned with the intended head motion vectors, though with smaller eye velocities compared to the other subjects. (C,F,I,L,O) Subject MVI004 produced selective eye movements for all tested vectors, save for stimuli targeting the LHRH axis (F) where an unintended LARP component grew in amplitude with the targeted horizontal eye movement.





1289  
 1290  
 1291  
 1292  
 1293  
 1294  
 1295  
 1296  
 1297  
 1298  
 1299  
 1300  
 1301  
 1302  
 1303  
 1304  
 1305

**Figure S6. Vestibulo-ocular reflex gain and phase during whole-body rotation in darkness.**

Mean±SD horizontal vestibulo-ocular reflex (VOR) gain and phase lead for 0.1/0.2/0.5/1/2 Hz 100°/s peak rotary chair testing of subjects MVI001 (A,B), MVI002 (C,D), MVI003 (E,F) and MVI004 (G,H), performed before implantation (*Pre-Op*, for all subjects except MVI001); 3 wk post-implantation, just before initial MVI activation (*Post-Op*); and at the most recent study visit (after 812, 738, 782 and 354 days of continuous stimulation, respectively) with MVI motion-modulation on (“MVI ON”) or with a placebo constant-rate stimulus (“modulation OFF”). Each data point is the cycle-averaged mean for n=2 to 32 (median 13) cycles. Phase was only computed for VOR responses >1.5°/s. Normative data range shown is from Wall et al. for 25 normal subjects age 50-69 years.(49) (A) For subject MVI001, who was not tested at 0.1/0.2/0.5/1/2 Hz pre-operatively, black x’s show pre-op data from a test at another institution prior to study enrollment. “MVI ON” VOR gain significantly exceeds “Modulation OFF” gain at every tested frequency (Wilcoxon rank sum test at each frequency: p<0.01) but is still below normal. (C) Subject MVI002’s MVI ON gain significantly increased vs. pre-op at 0.1-0.5Hz (p<0.05) but decreased at 1-2Hz (p<0.05). MVI ON gain exceeds modulation OFF gain at every frequency (p<0.001). (E) Subject MVI003’s MVI ON gain significantly increased vs. pre-op and vs. modulation OFF at every frequency (p<0.05). (B,D,F,H) Phase responses improved toward normal over 0.1-1Hz.

Implanted Canal		Left Posterior			Left Horizontal			Left Anterior			
Electrode		E3	E4	E5	E6	E7	E8	E9	E10	E11	
MVI001R019	Phase Duration ( $\mu$ s)	50	-	-	-	200	-	-	-	200	
	Current intensity level (%)	10%	350	-	-	-	220	-	-	-	349
		20%	368	-	-	-	243	-	-	-	368
		30%	387	-	-	-	267	-	-	-	392
		40%	406	-	-	-	290	-	-	-	415
		50%	425	-	-	-	326	-	-	-	439
		60%	444	-	-	-	378	-	-	-	458
		70%	463	-	-	-	425	-	-	-	481
		80%	481	-	-	-	472	-	-	-	505
		90%	500	-	-	-	519	-	-	-	529
100%	519	-	-	-	571	-	-	-	552		
MVI002R004	Phase Duration ( $\mu$ s)	100	100	200	100	100	200	100	200	-	
	Current intensity level (%)	10%	300	349	300	50	250	300	201	250	-
		20%	330	373	330	71	269	330	227	260	-
		30%	363	401	363	93	288	363	255	269	-
		40%	397	430	397	116	316	397	283	278	-
		50%	430	456	430	151	354	430	321	288	-
		60%	463	486	463	196	392	463	373	297	-
		70%	496	515	496	241	434	496	430	312	-
		80%	529	543	529	289	472	529	486	330	-
		90%	562	571	562	359	510	562	543	349	-
100%	599	599	599	448	552	599	599	373	-		
MVI003R140	Phase Duration ( $\mu$ s)	200	200	200	200	200	200	200	200	-	
	Current intensity level (%)	14%	200	201	300	448	349	300	201	151	-
		29%	241	219	345	481	396	345	208	168	-
		43%	283	241	396	514	448	396	217	184	-
		57%	349	262	448	548	500	448	224	200	-
		71%	429	283	495	581	548	496	235	217	-
		86%	514	307	548	623	599	548	241	234	-
		100%	599	349	599	699	699	599	250	250	-
MVI004R201	Phase Duration ( $\mu$ s)	200	200	200	200	200	200	200	200	200	
	Current intensity level (%)	14%	125	125	175	224	175	224	25	125	224
		29%	170	168	212	253	219	264	58	179	264
		43%	217	212	250	283	267	307	91	234	307
		57%	262	257	288	321	321	387	125	288	387
		71%	316	300	349	382	415	467	191	382	467
		86%	406	387	425	439	505	548	257	491	548
		100%	500	477	500	500	599	651	349	599	651

**Table S1. Pulse parameters used for current fitting experiments.**

Phase durations ( $\mu$ s) and current amplitudes ( $\mu$ A) used in fitting experiments (Figures 3, 4, S1 and S2) for all tested electrodes. Current intensity levels are expressed as fractions of the range from the current at which a subject first reported illusion of head movement to the maximum tolerated current. Each level was tested using 15-20 repetitions of 200 pulse/s pulse trains lasting 200 ms each and repeated every 500 ms. Subjects MVI003 and MVI004 were tested with only seven levels each due to time constraints.

1312

	<b>Subject ID</b>	<b>MVI001</b>	<b>MVI002</b>	<b>MVI003</b>	<b>MVI004</b>
	Date Implanted	9/7/2016	11/30/2016	2/23/2017	1/5/2018
	Ear implanted	Left	Left	Left	Left
<b>LARP</b>	Electrode	E3	E3	E3	E3
	Phase duration $\mu$ s	50	100	200	200
	Pulse current $\mu$ A	390	600	600	406
	Pulse Rate pulses/s [pps]	100	100	100	100
<b>LHRH</b>	Electrode	E7	E6	E6	E6
	Phase duration $\mu$ s	200	100	200	200
	Pulse current $\mu$ A	570	160	620	320
	Pulse Rate pps	100	100	100	100
<b>LARP</b>	Electrode	E11	E9	E9	E11
	Phase duration $\mu$ s	200	100	100	200
	Pulse current $\mu$ A	480	600	400	550
	Pulse Rate pps	100	100	100	100

1313  
 1314  
 1315  
 1316  
 1317  
 1318  
 1319

**Table S2. Electrical stimulation parameters used during device activation.**

Stimulation parameters used during initial device activation (onset of continuous stimulation) in all three canals for all subjects, corresponding to data in Figures 5 and S3. The table lists the active electrode contact number, phase duration, pulse amplitude, and stimulus pulse rate for each channel. At the time of initial activation, subjects were not yet acclimated to non-zero pulse rates. Continuous pulse rates representing zero head motion were subsequently increased to 150 pulse/s for subjects MVI002, MVI003 and MVI004 on all channels.



	Modulated Parameter	Subject ID	MVI001	MVI002	MVI003	MVI004
		Date of Testing	11/02/2016	1/24/2017	04/18/2017	02/27/2018
		Days Since Activation	56	55	54	53
		Electrode ID	E3	E3	E3	E3
RALP	Phase duration $\mu$ s	200	100	200	200	
		Electrode ID	E3	E3	E3	E3
	Current	Map Type	Flat	Linear	Flat	Linear
		Minimum current $\mu$ A	N/A	500	N/A	125
		Zero-motion current $\mu$ A	450	600	600	406
		Maximum current $\mu$ A	N/A	700	N/A	500
		Compression Factor	N/A	N/A	N/A	N/A
	Rate	Map Type	Sigmoidal	Sigmoidal	Sigmoidal	Sigmoidal
		Minimum pulses/s [pps]	0	0	0	0
		Zero-motion rate pps	100	150	150	150
Maximum rate pps		400	450	450	450	
Compression Factor		2	5	2	5	
LHRH	Phase duration $\mu$ s	200	100	200	200	
		Electrode ID	E7	E6	E6	E6
	Current	Map Type	Flat	Linear	Sigmoidal	Sigmoidal
		Minimum current $\mu$ A	N/A	150	610	220
		Zero-motion current $\mu$ A	600	350	620	320
		Maximum current $\mu$ A	N/A	550	700	470
		Compression Factor	N/A	N/A	20	3
	Rate	Map Type	Sigmoidal	Sigmoidal	Sigmoidal	Sigmoidal
		Minimum pulses/s	0	0	0	0
		Zero-motion rate pps	100	150	150	150
Maximum rate pps		400	450	450	450	
Compression Factor		2	5	2	5	
LARP	Phase duration $\mu$ s	200	100	100	200	
		Electrode ID	E11	E9	E9	E11
	Current	Map Type	Flat	Linear	Sigmoidal	Linear
		Minimum current $\mu$ A	N/A	500	400	220
		Zero-motion current $\mu$ A	700	600	400	550
		Maximum current $\mu$ A	N/A	700	420	600
		Compression Factor	N/A	N/A	20	N/A
	Rate	Map Type	Sigmoidal	Sigmoidal	Sigmoidal	Sigmoidal
		Minimum pulses/s [pps]	0	0	0	0
		Zero-motion rate pps	100	150	150	150
Maximum rate pps		400	450	450	450	
Compression Factor		2	5	2	5	

1320 **Table S3. MVI stimulation parameters for each subject during testing after 8-weeks of continuous, motion-**  
1321 **modulated electrical stimulation.** Stimulation parameters used by each subject's MVI for pulse-rate- and pulse-  
1322 amplitude-modulation at test session 8 weeks after activation (yielding data in Figures 6 and S4).

	Modulated Parameter	Subject ID	MVI001	MVI002	MVI003	MVI004	
		Date of Testing	10/29/2018	11/12/2018	03/27/2019	12/03/2018	
		Days Since Activation	812	738	782	354	
		Electrode ID	E3	E3	E3	E3	
<b>RALP</b>	Current	Phase duration $\mu$ s	200	100	200	200	
		Map Type	Flat	Linear	Flat	Linear	
	Rate	Minimum current $\mu$ A	N/A	500	N/A	125	
		Zero-motion current $\mu$ A	450	600	600	406	
		Maximum current $\mu$ A	N/A	700	N/A	500	
		Compression Factor	N/A	N/A	N/A	N/A	
	Rate	Map Type	Sigmoidal	Sigmoidal	Sigmoidal	Sigmoidal	
		Minimum pulses/s [pps]	0	0	0	0	
		Zero-motion rate pps	100	150	150	150	
		Maximum rate pps	400	450	450	450	
<b>LHRH</b>	Current	Compression Factor	5	5	5	5	
		Electrode ID	E7	E6	E7	E6	
	Rate	Phase duration $\mu$ s	200	100	200	200	
		Map Type	Flat	Linear	Sigmoidal	Sigmoidal	
		Minimum current $\mu$ A	N/A	150	350	220	
		Zero-motion current $\mu$ A	600	350	400	320	
	Rate	Maximum current $\mu$ A	N/A	550	620	470	
		Compression Factor	N/A	N/A	10	3	
		Map Type	Sigmoidal	Sigmoidal	Sigmoidal	Sigmoidal	
		Minimum pulses/s [pps]	0	0	0	0	
<b>LARP</b>	Current	Zero-motion rate pps	100	150	150	150	
		Maximum rate pps	400	450	450	450	
	Rate	Compression Factor	5	5	5	5	
		Electrode ID	E11	E9	E9	E11	
		Current	Phase duration $\mu$ s	200	100	200	200
			Map Type	Flat	Linear	Sigmoidal	Linear
	Rate	Minimum current $\mu$ A	N/A	500	180	220	
		Zero-motion current $\mu$ A	700	600	200	550	
		Maximum current $\mu$ A	N/A	700	300	600	
		Compression Factor	N/A	N/A	10	N/A	
Rate	Map Type	Sigmoidal	Sigmoidal	Sigmoidal	Sigmoidal		
	Minimum pulses/s [pps]	0	0	0	0		
	Zero-motion rate pps	100	150	150	150		
	Maximum rate pps	400	450	450	450		
Rate	Compression Factor	5	5	5	5		

**Table S4. MVI stimulation parameters for each subject during most recent test session**

Electrical stimulation parameters used by each subject's MVI for pulse-rate- and pulse-amplitude-modulation at the time of the most recent test session (yielding data in Figures 8 and S6).

1323  
1324  
1325  
1326

1327

1328 **Video S1. Evoked eye movements during manipulation of head worn unit on MVI004.**

1329 After 5 days of continuous, motion-modulation prosthetic electrical stimulation via electrodes in

1330 the three semicircular canal of the left ear, pitch rotation of subject MVI004's head worn unit

1331 (HWU) about the subject's +Y axis evokes compensatory vertical eye movements.